
Article:
Sparkes, J. orcid.org/0000-0002-1961-1384 and Holland, C. orcid.org/0000-0003-0913-2221 (2018) The rheological properties of native sericin. Acta Biomaterialia, 69. pp. 234-242. ISSN 1742-7061

https://doi.org/10.1016/j.actbio.2018.01.021

The rheological properties of native sericin

James Sparkes[a] and Chris Holland[a,*]

a) Department of Materials Science and Engineering, The University of Sheffield, Sir Robert Hadfield Building, Mappin Street, Sheffield, S. Yorks, S1 3JD, UK

Statement of Significance

This study addresses one of the major gaps in our knowledge regarding natural silk spinning by providing rigorous rheological characterisation of the other major protein involved – sericin. This allows progress in silk flow modelling, biomimetic system design, and in assessing the quality of bioinspired and waste sericin materials by providing a better understanding of the native, undegraded system.

Abstract

Unlike spider silk, spinning silkworm silk has the added intricacy of being both fibre and micron-thick glue-like coating. Whilst the natural flow properties of the fibre feedstock *fibroin* are now becoming more established, our understanding of the coating, *sericin* is extremely limited and thus presents both a gap in our knowledge and a hindrance to successful exploitation of these materials. In this study we characterise sericin feedstock in its native state from the silkworm *Bombyx mori*, and by employing both biochemical, rheological and spectroscopic tools, define a natural gold standard. Our results demonstrate that native sericin behaves as a viscoelastic shear thinning fluid, but that it does so at a considerably lower viscosity than its partner fibroin, and that its upper critical shear rate (onset of

gelation) lies above that of fibroin. Together these findings provide the first evidence that in addition to acting as a binder in the construction of the cocoon, sericin is capable of lubricating the flow of fibroin within the silk gland, which has implications for future processing, modelling and biomimetic efforts of these materials.

Keywords

Sericin; *Bombyx mori;* characterisation; rheology; FT-IR spectroscopy.

1. Introduction

In nature silks can be spun under ambient conditions to achieve a wide range of strength[1–6], elasticity[7–9] and toughness[1,8,10–14], inspiring many to try and replicate these materials industrially[15–23]. However, a major limiting factor in furthering our understanding of silk production is that while much has previously been published on the function, properties, and structure of the primary proteins responsible for the fibrillar structure of silks (*fibroins* in silkworms and *spidroins* in spiders)[19,24,25], much less is known about the secondary proteins. Whilst not responsible for the impressive mechanical properties of a silk fibre per se, in their natural environment they perform a diverse range of functions that effectively extend the phenotype of silk by imbuing additional functionality, such as non-woven composite formation[26–29], water retention[30] or even adhesive qualities[31].

In this study we focus on the group of secondary silk proteins produced by *Bombyx mori,* known as sericins, which act as the binder between brins and adjacent cocoon fibres in their spun state[8,27,29,32,33]. These proteins account for approximately 30% of the spun silk fibre[34], and thus represent a considerable resource investment for the silkworm, which pertains to their biological significance.

Sericins are water soluble, globular proteins[32,35]. They are most accurately described as a multi-component protein with an indefinite structure, which are secreted at various points along the gland, beginning in the middle posterior section[32,35–37]. These proteins have marginally different compositions, solubility, and levels of crystallinity[32,37]. However whilst we have insights into their structure, little is known about sericins' functions within the gland, with only suggestions or assumptions that they act as a lubricant for fibroin [38–41]. This may be in part due to the experimental difficulties in extracting and testing this material with minimal processing, as although fibroin can be

readily extracted in its native state from mature *B. mori* larvae[42], isolation of native sericin in a similar fashion has thus far proved problematic.

Large quantities of sericin solution are produced industrially from wastewater in the cocoon degumming process[43–45] and find uses in the food[46–48], cosmetic[32,49–52], biomedical[53–57], and health supplement industries[58]. Much of the recent work on sericins has focused on the extraction methods[32,59–62], characterisation of[48,59,63–68], and potential uses[32,51,55,62,69–73] for this by-product, with the primary aim of commercial diversification. Nevertheless, the combination of high temperature, pressure, and solvents typically used affects the quality of the sericin produced through changes to its conformation or molecular weight [32,35,57,63,73–76]Therefore, while these industrially derived sericins represent promising advances in their respective fields, and a significant waste reduction in traditional silk industries[32,60,61,74,77], the mechanical[78–81] and rheological[35,47,78,79,82–84] sericin characterisation undertaken in these studies cannot be considered truly representative of the natural system.

Looking towards alternative methods for sericin extraction, early studies suggested that sericin could be extracted through time limited dissolution of *B. mori* glands[34,84], however this has proven difficult to control, as it is subject to contamination from fibroin and requires re-concentration. Other techniques, such as surgically removing the posterior (fibroin producing) section of the gland and dissolution of the resultant fibroin deficient feedstock[85,86], have not gained traction in the silk community due to the time-consuming, complex, and invasive nature of the operation. The use of the standard LiBr fibroin reconstitution method[87] has been employed with mutant *B. mori* strains to dissolve sericin only cocoons[68,88], but this can hardly be considered less degrading than wastewater extraction methods.

To this end, we have opted to apply our existing techniques for native fibroin extraction[42,89] to a fibroin deficient strain of *B. mori* thus providing a ready source of native sericin feedstock without the need for several interim processing steps. To our knowledge there is only one study which details the rheological properties of native sericin taken from the glands of a fibroin deficient *B. mori* strain, but the number of samples (n=1) used, and the unlikely supposition that a polymer solution is a Newtonian fluid limits the applicability of this data[90]. Hence looking to extend our understanding of this area, we present rheological data obtained from large sample sizes in an attempt to gain fundamental insights into this material. This work seeks to define native sericins' processing parameters and provide baseline data to both further our investigations into the recently discovered pultrusion dominated spinning

mechanisms of silk (for it is pulled, not pushed from the body) [91], and address the major limitations identified in previous flow studies[38,39,42,92,93]. We show that sericin is a polymer solution which exhibits non-Newtonian, shear thinning behaviour; that its viscosity lies significantly lower than fibroin, and that its upper critical shear rate (onset of gelation) lies above that of fibroin. All of which allows us to conclude that native sericin can act as a lubricant as well as binding cocoon fibres.

2. Materials and methods

2.1. Silkworm rearing

Fibroin deficient *B. mori* silkworms (Nd-s strain, supplied by *Silkworm Genetic Resource Database*, Kyushu University, Japan) were raised over a period of 6 weeks on black mulberry (*Morus nigra)* and silkworm chow (Silkworm store, UK) in a temperature and humidity controlled environment (28°C, 80-85% RH, reduced to 26°C, 70-75% in the final instar). When worms were observed to have begun wandering (loss of appetite, increased motion, voiding (at later stages) they were transferred to a cool (10°C) environment to delay spinning.

The strain used has an incomplete penetrance of the phenotype responsible for the undeveloped posterior gland and resultant fibroin deficiency, meaning that not all silkworms of this strain produce sericin only. Identification of specimens carrying this phenotype was aided greatly by bimodal variation in their appearance (see **Figure 1**) – *Dark*, with a mottled body (dark grey patches over a pale grey-white) and *Light* – which were a uniform pale grey-white (similar to regular *B. mori*).

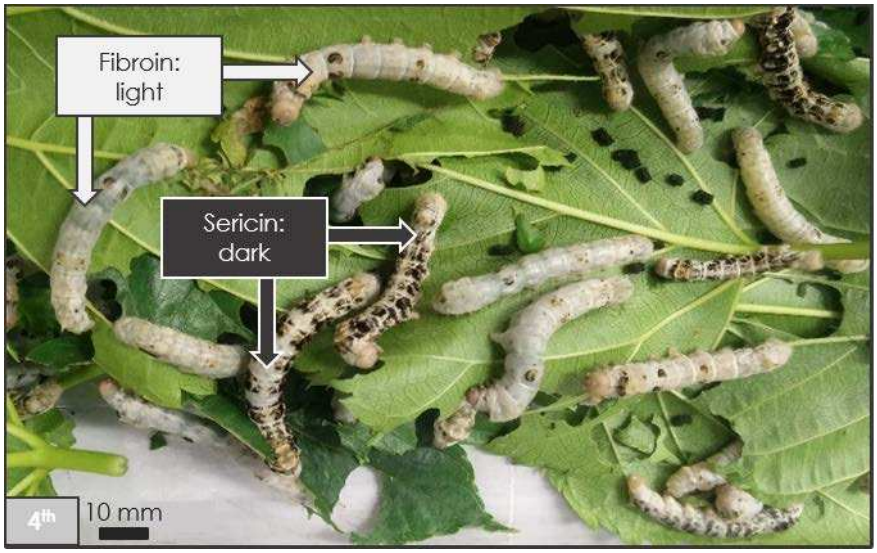

Figure 1: Identification of fibroin deficient Bombyx mori samples.

Individual sericin only mutants are readily identified through stark differences in patterning. Initially this was assumed to be variation in sex, but all colour pairings produced viable offspring. Confirmation of sericin/fibroin production is detailed in section 2.3. In keeping with this natural colouring, all future graphs use dark colours to represent sericin data and pale grey for fibroin.

2.2. Sample preparation

Feedstock was extracted from silk glands as per previously described fibroin extraction methods[42]. Adjacent portions of the same section of the middle division of the gland were used for rheological and concentration characterisation for all samples and assumed to be of equal concentration. Feedstock concentration was determined through evaporation to dryness and is expressed as mg/mg %.

2.3. Material identification

2.3.1. Spectroscopic characterisation

Attenuated Total Reflectance (ATR) Fourier-Transform Infra-Red (FT-IR) spectroscopy (Nicolet 380, Thermo Scientific, Waltham, USA) purged with dry air (118ml/s Parker Balston, UK) was performed on the same samples as those used for amino acid analysis. Samples were progressively scanned as they were evaporated to dryness using a vacuum chamber mounted above the ATR crystal to leave a thin film on the ATR crystal. Spectra were obtained between 800-4000 cm^{-1}, performing 64 scans at 4 cm^{-1} resolution and are presented after correction for background absorbance and ATR sampling depth, and normalised against the amide I peak.

2.3.2. Amino acid analysis

Gland contents were dissolved in type I water and submitted for analysis in the PNAC Facility at the University of Cambridge. Samples were hydrolysed with 250 nmol norleucine standard, with 1% of the sample analysed using ion exchange liquid chromatography, and post column derivatisation achieved using ninhydrin (Biochrom 30, Biochrom, Cambourne, UK).

2.3.3. Molecular weight determination

Gland contents were dissolved in type I water, diluted to 0.1 and 0.05% (mg/mg) and reduced with an equal volume of 4% (mg/mg) SDS in 4 mM 2-mercaptoethanol. Gel electrophoresis was used to determine the molecular weights (MW) of the proteins in each sample. An SDS-PAGE system comprising a 4-20% poly-acrylamide gel was run in ambient conditions at 160V, 100mA, using an Amersham ECL Gel kit (GE Healthcare, Chicago, USA). A high molecular weight ladder ranging 30- 460kDa (HiMark, ThermoFisher Scientific, Waltham, USA) was used as the protein standard. Gels were fixed and scanned at high resolution (1200 dpi) using a photo scanner (HP Scanjet G2710). Pixel intensity was measured as a function of distance along each lane using ImageJ94, and normalised against full lane length to allow comparison across lanes and determination of MWs.

2.4. Rheological characterisation

Rheological testing was carried out on a Bohlin Gemini rheometer (Malvern Instruments, UK) equipped with a Peltier stage and moisture trap for temperature and humidity control. Experiments were performed using the CP1/10 cone and plate geometry (10 mm diameter, 1° cone, 30 µm truncation gap). After dissection, extreme care was taken to minimise loading whilst placing the samples onto the static plate before lowering the cone onto the sample to ensure a completely filled gap. In order to avoid skin formation at the sample-air interface affecting the results, the sample was flooded with a minimal sheath of water, which was maintained throughout each experiment[42].

Specimens were subjected to a period (100 s) of pre-shear (1 s^{-1}) to improve sample homogeneity between the plates[42,93–95]. Apparent viscosity measurements were made by averaging the final 30 s of this test. Afterwards an oscillatory sweep from 25 - 0.1 Hz at an applied strain of 0.02 (below the material's linear viscoelastic limit) was performed to ensure that the sample had not gelled (presence of a crossover from viscous to elastic modulus as the dominant response) before principal testing commenced.

Principal tests either took the form of a shear ramp (ranging from 0.01 - 300 s^{-1}) followed by a further oscillatory sweep to confirm gelation, or a temperature ramp at a fixed frequency (0.1 Hz) and strain (0.02) at 1°C.min^{-1} from 25°C, down to 2°C, up to 80°C, where a second oscillatory sweep was performed before finally returning to 25°C and a final oscillatory sweep. Some test runs incorporated slight variations in this sequence, in order to better probe the material properties. The reference samples presented show the traits discussed with the highest clarity, while samples showing unusual viscoelastic responses (such as stress overshoot, ejection, or skin formation) were discarded from our analysis (full set of data is available via ORDA[96]).

For viscosity measurements Carreau Yasuda fitting was performed by first trimming the data at the lowest shear rate region to remove data influenced by excess instrument noise. The upper shear rate regime was curtailed beyond $\dot{\gamma}_{UC}$ (determined as the point at which the normal force begins to rise rapidly, minimum viscosity and gelation begins). Model parameters were estimated to provide starting values for MatLab's curve fitting toolbox. Goodness of fit was assessed using Escudier's[97] modified sum of squares approach, which provides a better fit across the wide range of shear rates. The severity and influence of outliers were identified through the combined use of Student's T and Cook's Distance/DFFits tests, with those ranking highly in both aspects removed from the data sets if found to exert significant influence on the goodness of fit.

2.5. Statistical Analysis

Data is presented as the mean ± standard deviation and based on *n* repeats. Significant difference between samples was determined by an unpaired t-test with a two tailed P value of $P<0.0001$.

3. Results and discussion

The first requirement was to determine that silkworm specimens were producing the anticipated native sericin feedstock. Natural, biological, variation was minimised by using samples from the same batch at the same life cycle stage. After feedstock extraction, we performed several experiments on the native samples to confirm their composition - amino acid analysis, gel electrophoresis data (see supporting information) and FT-IR (see **Figure *2***) agree that *Dark* specimens produce a fibroin deficient silk feedstock consisting primarily of sericin, while *Light* specimens produce a regular fibroin feedstock.

Our findings are consistent with previous studies of this strain, where fibroin deficient individuals produce a native feedstock that is composed of ~98.5% sericin [102] of molecular weights 24-400 kDa [37,99–101]. Given we are primarily interested in the rheological properties of sericin, beyond confirmation of sericin presence, *Light* specimens also serve as a useful internal control, and their feedstocks are consistent with regular *B. mori* fibroin[17,42,89,93–95,98]. Hereafter, when we discuss native sericin's properties, these relate to samples from the *Dark* specimens, whereas native fibroin's properties are gleaned from Light specimens and the wider literature.

There are of course several limitations and assumptions made in our approach to characterising a fibroin deficient/native sericin feedstock, however we have taken the same approach to native feedstock rheology as in previous studies [89,42,40,92,90] and assume a native proteins' contribution to the bulk viscoelastic properties, is a product of its molecular weight and abundance and that the minor protein constituents of a silk feedstock are likely to play a less dominant role in the bulk rheological properties [103,104].

As a final comment on sample impurity, given our principal aim of determining the ability of the sheath proteins to lubricate the flow of fibroin during natural spinning, it seems appropriate to assess the native feedstock as a whole, rather than purification to 100% sericin, as it better represents the natural system.

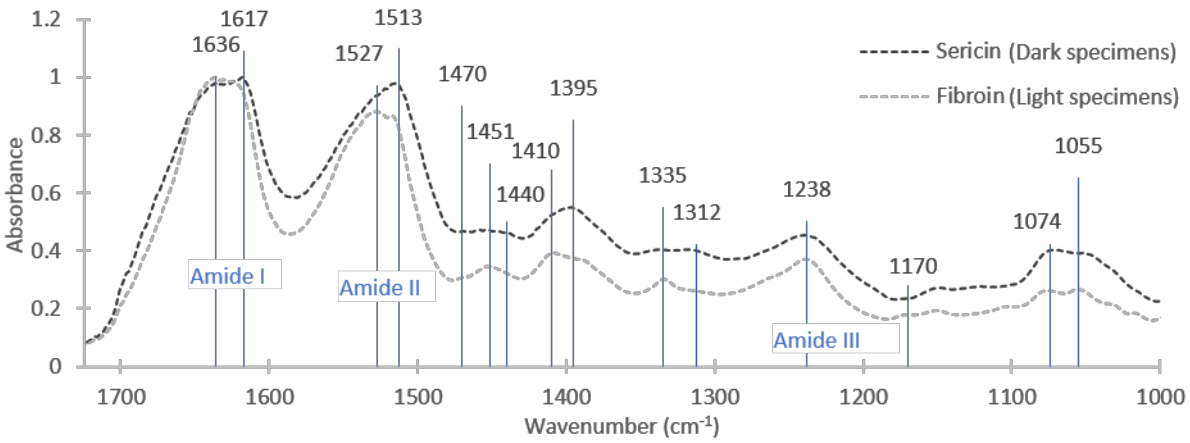

Figure 2 Sericin and fibroin FT-IR spectra

Spectra (normalised against amide I peak) of native sericin (dark specimens) compared to fibroin (light specimens) shows distinct differences. Peaks used in the identification of each protein are labelled with their respective wavenumber. Of further note the native sericin presented here provides a "gold standard" for comparison of processed sericin materials against the native system. For further details on assignments, see supplementary table 2.

Beyond our confirmatory experiments above, comparison between sericin and fibroin feedstocks revealed significant concentration differences between the two (**Figure *3***).Fibroin specimens show a mean concentration of ~ 21%, marginally lower than that reported by Laity *et al.*[42], but within their expected range. However, the sericin samples show a considerably lower mean of ~13%, albeit with a similar level of spread, which is consistent with previous measures of sericin concentration (14%)[90,93].

Not only are there differences in concentration between feedstocks, we also observed differences in their rheological properties. As shown in **Figure *3***, sericin appears to offer a broad range of apparent viscosities, from 4-220 Pa.s and a mean of approximately 40 Pa.s - two orders of magnitude below that of fibroin (our fibroin mean was 1931 Pa.s, comparable to Laity's 1722 Pa.s[42]). When concentration is accounted for we find that for a given concentration of feedstock, sericin has a considerably lower viscosity than fibroin, despite their reportedly similar molecular weights[99] (See supplementary figure 1). Furthermore, unlike typical polymer solutions, both sericin and fibroin viscosity show little overall correlation with concentration, agreeing with previous observations of fibroin (see **Figure *3***)[93].

Taken together these results suggest variations in viscosity may be due to compositional and conformational differences of the proteins moderating the level of intermolecular friction/interaction. Although structural studies of sericin[85,105] and fibroin[106–110] suggest that they both exhibit random coil conformations in solution, in sericin, the combination of longer side chains[42], and an increased hydrophilic amino acid fraction[42] (53 vs. 19 mol%) present a protein that although exhibiting random coil behaviours, has a greater affinity to water than itself, resulting in a weaker gel formation in its native aqueous solution.

Probing the gel properties of sericin further, oscillatory sweeps were used to determine the viscoelastic response of the feedstocks, with both sericin and fibroin behaving as weak gels[111–114]. However, as can be seen in **Figure 4**a, the bimodal distribution of crossover points shows that there are clear differences between sericin (crossover frequency ω_X = 10±5 Hz; crossover modulus G_x = 482±326 Pa) and fibroin feedstocks (ω_X = 0.58±0.47 Hz; G_x = 2906±1297 Pa), with the former showing a greater viscous response and substantially lower modulus, whilst the latter provides further evidence that *Light* specimens produce fibroin, with mean crossover values similar to previously published work[17,42,89,115–117]. In the case of sericin feedstocks, the presence of a shorter relaxation time (estimated as $1/\omega_X$), and a larger lower critical shear rate ($\dot{\gamma}_{LC}$, which marks the rate at which the transition between

207 Newtonian and power law behaviour can be said to occur, is numerically equivalent to ω_X) identifies a more liquid-like

208 behaviour which remains Newtonian until higher shear rates are encountered.

209

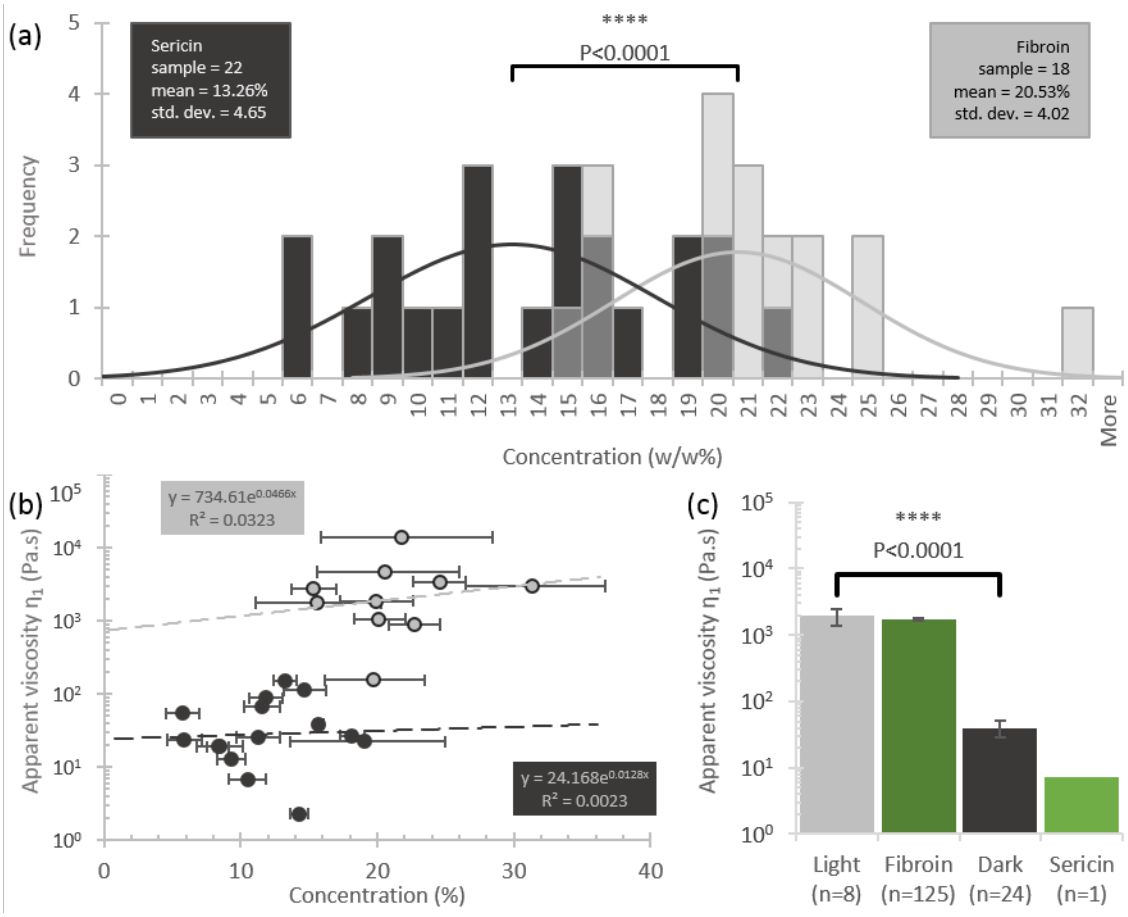

Figure 3: Sericin concentration and apparent viscosity determination

(a) *- Empirical (bars) and probability (curves) density functions for concentration of fibroin and sericin feedstocks. For the probability density functions, P<0.0001.* ***(b)*** *- Plotting viscosity against concentration shows very little correlation between the two factors for sericin (●) or fibroin (○). Horizontal error bars represent the variation due to measurement uncertainty due to small sample sizes.* ***(c)*** *– Mean apparent viscosity for samples compared with literature values for fibroin and sericin. An unpaired t-test with a two tailed P value of P<0.0001 suggests extreme statistical significance.*

Fitting a binary Maxwell model (a la Laity et al[42]) to the data suggests the presence of two relaxation modes in sericin feedstocks, at around 1.22 and 0.02 s, which are of similar magnitude to relaxation modes 3 and 4 reported for fibroin[93–95] (For calculations see supplementary materials). Furthermore, normalisation of the oscillatory data with respect to each sample's crossover point[93], demonstrates the consistency of the fibroin feedstocks (**Figure 4**b) and the apparent variation in properties of sericin feedstocks (**Figure 4**c). This consistency has been hypothesised to be related to a feedstock's molecular weight distribution, thus our results are consistent with reports that while fibroin's production is relatively consistent, there are up to 7 different sericin proteins[99,118–120] secreted into the gland in quantities that vary on a specimen by specimen basis[101,120], with molecular weights ranging from 24 to 400 kDa [37,99–101].

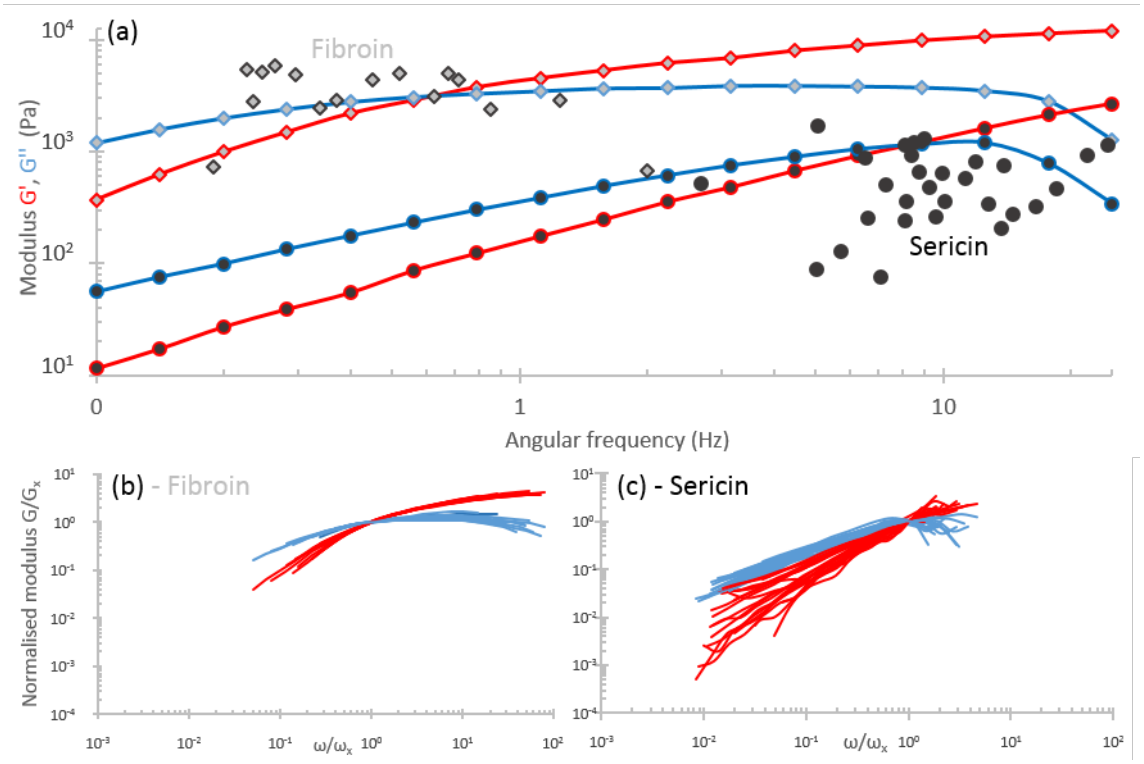

Figure 4: The frequency dependence of sericin

***(a)** - Variability in the frequency response of samples is shown by plotting the crossover points for Sericin (●, conc. 13.3%) and fibroin (◇, conc. 20.5%). The two sets of oscillatory data (elastic, —; viscous, —) are representative of the viscoelastic response of sericin and fibroin. The presence of a bimodal distribution shows that there are distinct viscoelastic responses from each group, with sericin's reaction remaining in the viscous domain much until much higher frequencies than fibroin. **(b,c)** - Normalising modulus and frequency data against crossover modulus and frequency reveals master curve alignment in fibroin **(b)** and sericin **(c)** specimens. The greater level of spread shown by sericin indicates variation in the molecular weight distribution attributable to the less conserved nature of sericin production compared to fibroin.*

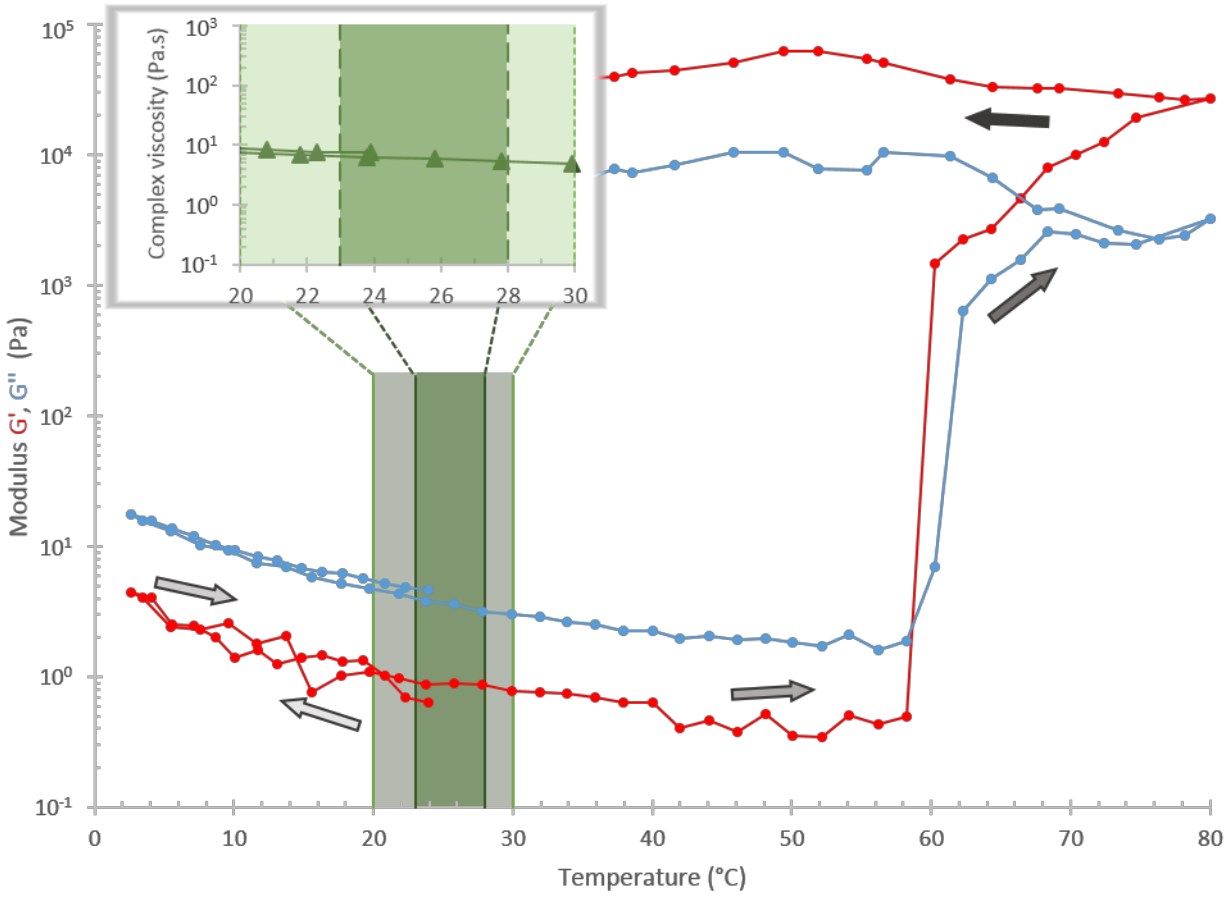

238

Figure 5: The effect of temperature on sericin

*Representative response of a single sericin sample (conc. 15.7%) subjected to temperature sweep under steady oscillation (0.1 Hz). First from 25°C to 2°C, then 80°C, where a frequency sweep was undertaken, before returning to 25°C. A minor reversible increase occurs in both elastic (●) and viscous (●) moduli in response to reduced temperature. A steady reduction is observed until a sudden take off in both moduli occurs, marking the transition to an elastic dominated regime. Further conversion is observed during the latter stages of the temperature sweep (increased moduli), with the gel formed shown to be strong (plateau G', G'') and permanent (G'>G''). Background colours depict the preferred (■) and possible (■) rearing temperatures. **Inset** panel shows the relative invariance of the complex viscosity across the range of viable spinning temperatures, suggesting that spinning is not dependent on temperature.*

239

240

We conducted temperature sweeps between 2 and 80 °C in order to explore the effect on sericin's flow properties across a range of natural and unnatural spinning temperatures. Sericin shows a typical protein response to elevated temperatures (see **Figure *5***), denaturing permanently into a strong gel (indicated by rapid increase in both moduli, and the temperature independent frequency response after reaching this temperature) at approximately 60°C. The most productive rearing temperatures for *B. mori* lie between 23 and 28 °C, though a range between 20 and 30 °C is commercially viable. Outwith this range, silkworm health deteriorates and is thus undesirable[121]. The inclusion of complex viscosity measurements in **Figure *5*** allows the appreciation that over the course of the natural spinning range, it is relatively invariant.

In order to probe sericin's flow response to at shear rates encountered during silk spinning[91], shear rate ramps were applied to samples (**Figure *6***). All samples were found to exhibit shear-thinning behaviour expected of concentrated polymer solutions, with the transition from Newtonian to shear thinning regime occurring above the lower critical shear rate region for sericin samples (mean = 10 s^{-1}, which is comparable to the only previously reported[122] value of 3 s^{-1}). At higher shear rates a distinct change in viscosity is accompanied by a change in shear stress and normal force (see **Figure *6***). Drawing on previous work into fibroin rheology[17,42,89,93,95,116,123], this upper critical shear rate ($\dot{\gamma}_{UC}$) is that at which the onset of shear induced gelation occurs within the sample. Here a general trend can be observed that the critical shear rate $\dot{\gamma}_{UC}$ varies inversely with the apparent viscosity η_1, with lower viscosities relating to higher upper critical shear rates.

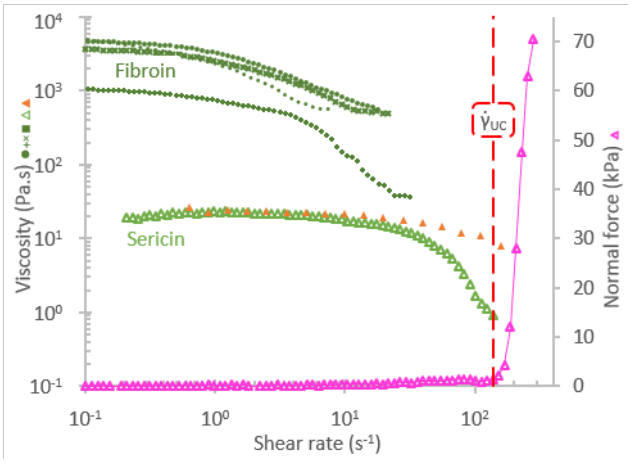

259

Figure 6: – The viscosity-shear rate relation for sericin

Comparing sericin's (conc. 11.3%) dynamic (△) and complex (▲) viscosities via the Cox-Merz relationship shows high correlation at low shear rates/angular frequencies, but divergence above this, with the measured dynamic viscosity exhibiting much stronger shear thinning behaviour than Cox-Merz predicts, suggesting unequally[127] *weighted polydispersity*[124]*. The normal force (△) response to the shear ramp is also shown on the secondary axis, along with the upper critical shear rate (— —). The rapid increase in normal force at this point represents the sudden rise in elasticity due to shear-induced gelation. For ease of comparison, several fibroin shear-ramps (conc. 15.3-24.6%), with zero shear viscosities across a broad range are shown (●, ×, ●, +). The final point in each represents the upper critical shear rate (gelation onset), and all of which are in the region where sericin is still acting effectively as a Newtonian fluid.*

260

261

More insight can be gained by interpreting our viscosity data using the Carreau-Yasuda model[124] (see methods), which has been shown to accurately depict a wide range of shear–thinning behaviours in polymer solutions. Variables fitted to individual specimens showed considerable variation in both the extent, and the rate of shear thinning. Comparisons were made between experimentally measured apparent viscosity and the modelled zero shear viscosity, with a high degree of correlation ($R^2 = 0.98$) between the two. This allows further simplification of the Carreau-Yasuda model by reducing the number of parameters to 3 (relaxation time, shear thinning rate, and transition breadth) which improves model validity.

Model fitting parameters are shown in Table 1. General trends that can be observed include that the rate of shear thinning and lower critical shear rate are inversely proportional to the zero shear viscosity, and that transition breadth rises in line with zero shear viscosity. We suggest that this may indicate that it is possible to infer sericin's shear response from its zero shear viscosity alone. A further observation is that despite the wide range of η_0 encountered for sericin, the proportional reduction in viscosity (η_{min}) remains roughly constant at approximately 80%. Fibroin was also observed to undergo a similar reduction of 90%, suggesting that whilst sericin does exhibit shear thinning behaviour, it is to a lesser extent than fibroin.

As explained above, whilst it is not currently possible to directly compare fibroin and sericin rheological properties from the same animal, considering our rheological data as a whole, we propose that for a typical non-fibroin deficient silkworm, the upper critical shear rate $\dot{\gamma}_{UC}$ for sericin gelation must only be higher than that of its fibroin (0.1 to 10 s^{-1},[39,40,89,92,115,116,123,125]), else sericin would aggregate before fibroin and inhibit fibre formation. Therefore the natural constraint on the system is simply to ensure that sericin has a greater upper critical shear rate than fibroin ($\dot{\gamma}_{UC,Fib} < \dot{\gamma}_{UC,Ser}$). With this in mind sericin may not have undergone as strong a selection to gel during the natural spinning process, which may be responsible for the wider variation in rheological properties.

Furthermore, we observe that sericin flows in a quasi-Newtonian manner throughout the fibroin shearing range (i.e. until $\dot{\gamma}_{UC,Fib}$), at which point its viscosity drops, which may be the result of selection for the need to maintain the consistent sericin-fibroin interface required for stable long-term fibroin storage[126], but later thin in order to ease the transport of an increasingly solid fibroin core through our recently proposed "solidity gradient" model[91]. These arguments are further supported by recent work into drying rates of newly spun fibres which found that the external

288 (sericin) layers remain wet for several seconds[116], and that when spun under high humidity, flow can continue
289 between cocoon layers[33], suggesting sericin does not solidify within the animal.

290

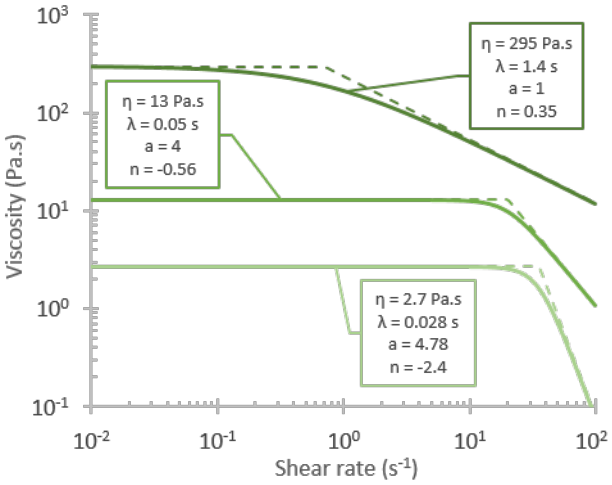

Figure 7: Shear dependent viscosity models for sericin

Exemplar shear response curves calculated from fitting the Carreau-Yasuda model to sericin samples shows the variation present. Solid lines indicate the best fit to the data, while the dashed lines have an instant transition from Newtonian to power law behaviour in order to appreciate the variation in the upper critical shear rate.

4. Conclusions

In conclusion, mottled specimens of the fibroin deficient W14 strain of *B. mori* are a good source of large quantities of unadulterated native sericin and this work provides a new standard for use in assessing the quality of recovered or reconstituted sericin. We have also shown that sericin's response to temperature changes is in line with other protein solutions, exhibiting extensive, rapid permanent denaturation above 60°C.

As with fibroin, sericin's viscosity varies across several orders of magnitude, but despite their similar molecular weights, these ranges barely overlap, with sericin occupying a much lower viscosity domain in the region of 1-250 Pa.s, whilst fibroin ranges from 200-10000 Pa.s. Given this, we ask whether, in terms of their shear response behaviour, they could be considered as part of a single spectrum.

The Cox-Merz relation has been shown to not be particularly applicable, as while the zero-shear viscosities are comparable, it systematically underrepresents the rate of shear-thinning at higher shear rates. Furthermore, native sericin is more readily shear thinning, has a lower initial viscosity, and a higher upper critical shear rate than native fibroin, all of which combine to provide a solution capable of providing a lubricating effect on the flow of fibroin. As a final observation, since apparent viscosity relates to zero shear viscosity, and as relaxation time, transition breadth, and shear thinning all relate to this, then we suggest that we may be able to **predict** sericin's shear response from apparent viscosity measurements alone, which would remove the need for destructive rheological testing.

312 *Table 1 - Summary of rheological results for native sericin solutions extracted from final instar B. mori silkworms*

Measurement method	Physical property	Mean	Standard deviation	Sample size *n*
Gravimetry	concentration (% mg/mg)	13.26 %	4.65	22
Steady shear	Apparent viscosity η_1	39.57 Pa.s	53.96	24
Oscillatory sweep	Crossover frequency ω_X	10.48 Hz	5.01	29
	Crossover Modulus G_X	482.14 Pa	325.63	
	Relaxation time $1/\omega_X$	0.019 s	0.010	
Temperature sweep	Gelation temperature	63.86 °C	8.16	3
Carreau-Yasuda model	Relaxation time λ_{CY}	0.51 s	0.44	14
	Zero shear viscosity $\eta_{0,CY}$	55.66 Pa.s	87.52	
	Parameter *a*	3.85	3.17	
	Parameter *n*	0.05	2.61	
	$\dot{\gamma}_{LC,Ser}$	10.09 s^{-1}	15.3	
	$\dot{\gamma}_{UC,Ser}$	58.47 s^{-1}	50.85	
Binary Maxwell model	Modulus contribution g_1	44.89 Pa	61.64	22
	Modulus contribution g_2	888.98 Pa	723.00	
	Relaxation time τ_1	1.22 s	1.86	
	Relaxation time τ_2	0.02 s	0.01	
	Zero shear viscosity $\eta_{0,BM}$	46.59 Pa.s	49.07	

313

In summary, we present evidence for the rheological properties of native sericin which is used to support the oft repeated, but previously unsupported, argument that in addition to acting as a binder within the cocoons, sericin performs a lubricating role in its liquid phase within the gland.

5. Acknowledgements

The authors would like to thank Dr Pete Laity for the helpful discussions, Dr Peter Sharratt for the amino acid analysis, and Professor Yutaka Banno and Tsuguru Fujii for providing the silkworm eggs. This work was supported by the EPSRC (EP/K005693/1) and the University of Sheffield.

5.1. Author information

5.2. Affiliations

The Natural Materials Group, Room J12, Department of Materials Science and Engineering, The University of Sheffield, Hadfield Building, Mappin Street, Sheffield, S. Yorkshire, UK.

James Sparkes and Chris Holland

5.3. Contributions

JS developed the hypotheses undertook experimental work and performed data analysis. CH provided further insight into the discussion. Both authors contributed to the writing and editing of the manuscript.

5.4. Disclosures

The authors declare no competing financial interests.

5.5. Corresponding author

Correspondence to Chris Holland (e-mail: *christopher.holland@sheffield.ac.uk*)

5.6. Supplementary materials

Supplementary information and raw datasets are available online.

6. References

[1] J.M. Gosline, M.E. DeMont, M.W. Denny, The structure and properties of spider silk, Endeavour. 10 (1986) 37–43. doi:10.1016/0160-9327(86)90049-9.

[2] F. Vollrath, Strength and structure of spiders' silks., J. Biotechnol. 74 (2000) 67–83. doi:10.1016/S1389-0352(00)00006-4.

[3] F. Vollrath, Biology of spider silk, Int. J. Biol. Macromol. 24 (1999) 81–88. doi:10.1016/S0141-8130(98)00076-2.

[4] D. Porter, F. Vollrath, Silk as a biomimetic ideal for structural polymers, Adv. Mater. 21 (2009) 487–492. doi:10.1002/adma.200801332.

[5] H.-P. Zhao, X.-Q. Feng, H.-J. Shi, Variability in mechanical properties of Bombyx mori silk, Mater. Sci. Eng. C. 27 (2007) 675–683. doi:10.1016/j.msec.2006.06.031.

[6] B. Madsen, Z. Shao, F. Vollrath, Variability in the mechanical properties of spider silks on three levels: Interspecific, intraspecific and intraindividual, Int. J. Biol. Macromol. 24 (1999) 301–306. doi:10.1016/S0141-8130(98)00094-4.

[7] B. Mortimer, C. Holland, F. Vollrath, Forced reeling of bombyx mori silk: Separating behavior and processing conditions, Biomacromolecules. 14 (2013) 3653–3659. doi:10.1021/bm401013k.

[8] B. Mortimer, J. Guan, C. Holland, D. Porter, F. Vollrath, Linking naturally and unnaturally spun silks through the forced reeling of Bombyx mori, Acta Biomater. 11 (2015) 247–255. doi:10.1016/j.actbio.2014.09.021.

[9] Y. Termonia, Molecular Modeling of Spider Silk Elasticity, Macromolecules. 27 (1994) 7378–7381. doi:10.1021/ma00103a018.

[10] I. Su, M.J. Buehler, Nanomechanics of silk: the fundamentals of a strong, tough and versatile material, Nanotechnology. 27 (2016) 302001. doi:10.1088/0957-4484/27/30/302001.

[11] A. Nova, S. Keten, N.M. Pugno, A. Redaelli, M.J. Buehler, Molecular and nanostructural mechanisms of deformation, strength and toughness of spider silk fibrils, Nano Lett. 10 (2010) 2626–2634. doi:10.1021/nl101341w.

[12] F. Vollrath, D. Porter, Silks as ancient models for modern polymers, Polymer (Guildf). 50 (2009) 5623–5632. doi:10.1016/j.polymer.2009.09.068.

[13] D. Porter, J. Guan, F. Vollrath, Spider silk: Super material or thin fibre?, Adv. Mater. 25 (2013) 1275–1279. doi:10.1002/adma.201204158.

[14] F. Vollrath, B. Madsen, Z. Shao, The effect of spinning conditions on the mechanics of a spider's dragline silk., Proc. Biol. Sci. 268 (2001) 2339–2346. doi:10.1098/rspb.2001.1590.

[15] A. Seidel, O. Liivak, L.W. Jelinski, Artificial Spinning of Spider Silk, Macromolecules. 31 (1998) 6733–6736. doi:10.1021/ma9808880.

[16] A. Rising, Spider Dragline Silk: Molecular Properties and Recombinant Expression, Swedish University of Agricultural Sciences, 2007.

[17] C. Holland, A.E. Terry, D. Porter, F. Vollrath, Natural and unnatural silks, Polymer (Guildf). 48 (2007) 3388–3392. doi:10.1016/j.polymer.2007.04.019.

[18] C. Holland, F. Vollrath, A.J. Ryan, O.O. Mykhaylyk, Silk and synthetic polymers: Reconciling 100 degrees of separation, Adv. Mater. 24 (2012) 105–109. doi:10.1002/adma.201103664.

[19] D.N. Breslauer, D.L. Kaplan, Silks: Properties and uses of natural and designed variants, Biopolymers. 97 (2012) 319–321. doi:10.1002/bip.22007.

[20] N. Dinjaski, D. Ebrahimi, S. Ling, S. Shah, M.J. Buehler, D.L. Kaplan, Integrated Modeling and Experimental Approaches to Control Silica Modification of Design Silk-Based Biomaterials, ACS Biomater. Sci. Eng. (2016) acsbiomaterials.6b00236. doi:10.1021/acsbiomaterials.6b00236.

[21] Z. Zheng, S. Guo, Y. Liu, J. Wu, G. Li, M. Liu, X. Wang, D.L. Kaplan, Lithium-free processing of silk fibroin, J. Biomater. Appl. 0 (2016) 1–14. doi:10.1177/0885328216653259.

[22] Y. Zhang, C. Zhang, L. Liu, D.L. Kaplan, H. Zhu, Q. Lu, Hierarchical charge distribution controls self-assembly process of silk in vitro, Front. Mater. Sci. (2015) 1–10. doi:10.1007/s11706-015-0314-8.

[23] T.R. Scheibel, Spider silks: recombinant synthesis, assembly, spinning, and engineering of synthetic proteins, Microb. Cell Fact. 3 (2004) 14. doi:10.1186/1475-2859-3-14.

[24] A.A. Walker, C. Holland, T.D. Sutherland, More than one way to spin a crystallite: multiple trajectories through liquid crystallinity to solid silk, Proc. R. Soc. B Biol. Sci. 282 (2015) 2–9. doi:10.1098/rspb.2015.0259.

[25] J.G. Hardy, L.M. Römer, T.R. Scheibel, Polymeric materials based on silk proteins, Polymer (Guildf). 49 (2008) 4309–4327. doi:10.1016/j.polymer.2008.08.006.

[26] F. Chen, D. Porter, F. Vollrath, Silk cocoon (Bombyx mori): Multi-layer structure and mechanical properties, Acta Biomater. 8 (2012) 2620–2627. doi:10.1016/j.actbio.2012.03.043.

[27] F. Chen, D. Porter, F. Vollrath, Silkworm cocoons inspire models for random fiber and particulate composites, Phys. Rev. E - Stat. Nonlinear, Soft Matter Phys. 82 (2010) 1–6. doi:10.1103/PhysRevE.82.041911.

[28] F. Chen, D. Porter, F. Vollrath, Structure and physical properties of silkworm cocoons, J. R. Soc. Interface. 9 (2012) 2299–308. doi:10.1098/rsif.2011.0887.

[29] F. Chen, D. Porter, F. Vollrath, Morphology and structure of silkworm cocoons, Mater. Sci. Eng. C. 32 (2012) 772–778. doi:10.1016/j.msec.2012.01.023.

[30] H. Elettro, S. Neukirch, A. Antkowiak, F. Vollrath, Adhesion of dry and wet electrostatic capture silk of uloborid spider, Naturwissenschaften. 102 (2015) 41. doi:10.1007/s00114-015-1291-6.

[31] A.A. Walker, S. Weisman, H.E. Trueman, D.J. Merritt, T.D. Sutherland, The other prey-capture silk: Fibres made by glow-worms (Diptera: Keroplatidae) comprise cross-??-sheet crystallites in an abundant amorphous fraction, Comp. Biochem. Physiol. Part - B Biochem. Mol. Biol. 187 (2015) 78–84. doi:10.1016/j.cbpb.2015.05.008.

[32] P. Aramwit, T. Siritientong, T. Srichana, Potential applications of silk sericin, a natural protein from textile industry by-products, Waste Manag. Res. 30 (2012) 217–224. doi:10.1177/0734242X11404733.

[33] C. Offord, F. Vollrath, C. Holland, Environmental effects on the construction and physical properties of Bombyx mori cocoons, J. Mater. Sci. (2016). doi:10.1007/s10853-016-0298-5.

[34] M. Tsukada, T. Komoto, T. Kawai, Conformation of Liquid Silk Sericin, Polym J. 6 (1979) 503–505.

[35] H.-Y. Wang, Y.-Q. Zhang, Effect of regeneration of liquid silk fibroin on its structure and characterization, Soft Matter. (2013) 138–145. doi:10.1039/c2sm26945g.

[36] Y.J. Wang, Y.Q. Zhag, Three-Layered Sericins around the Silk Fibroin Fiber from Bombyx mori Cocoon and their Amino Acid Composition, Adv. Mater. Res. vols 175-1 (2011) pp.158-163. doi:10.4028/www.scientific.net/AMR.175-176.158.

[37] S. Tokutake, Isolation of the smallest component of silk protein., Biochem. J. 187 (1980) 413–417.

[38] D.N. Breslauer, L.P. Lee, S.J. Muller, Simulation of Flow in the Silk Gland, Biomacromolecules. 10 (2009) 49–57. doi:10.1021/bm800752x.

[39] M. Moriya, K. Ohgo, Y. Masubuchi, T. Asakura, Flow analysis of aqueous solution of silk fibroin in the spinneret of Bombyx mori silkworm by combination of viscosity measurement and finite element method calculation, Polymer (Guildf). 49 (2008) 952–956. doi:10.1016/j.polymer.2007.12.032.

[40] M. Moriya, F. Roschzttardtz, Y. Nakahara, H. Saito, Y. Masubuchi, T. Asakura, Rheological properties of native silk fibroins from domestic and wild silkworms, and flow analysis in each spinneret by a finite element method, Biomacromolecules. 10 (2009) 929–935. doi:10.1021/bm801442g.

[41] K. Kataoka, Studies on silk fibroin III - on the liquid silk in silkgland, Kobunshi Ronbunshu. 32 (1975) 653–659. doi:10.1295/koron.32.653.

[42] P.R. Laity, S.E. Gilks, C. Holland, Rheological behaviour of native silk feedstocks, Polymer (Guildf). 67 (2015) 28–39. doi:10.1016/j.polymer.2015.04.049.

[43] B.Y. Keizo, the Preparation and Physico- Chiemical Properties of Sericin, [Book]. (1926) 1208–1223.

[44] L.J. ZHU, M. ARAI, K. Hirabayashi, Gelation of silk sericin and physical properties of the gel, J. Sericultural Sci. Japan. 64 (1995) 420–426.

[45] K. Hayasi, J. Oda, Light scattering by sericin solution (Part 1), Sci. Bull. Fac. Agric. Kyushu Univ. 16 (1957) 239–246. doi:10.15017/21433.

[46] T. Takechi, Z.-I. Maekawa, Y. Sugimura, Use of Sericin as an Ingredient of Salad Dressing, Food Sci. Technol. Res. 17 (2011) 493–497. doi:10.3136/fstr.17.493.

[47] L.C.B. Züge, V.R. Silva, F. Hamerski, M. Ribani, M.L. Gimenes, a. P. Scheer, Emulsifying Properties of Sericin Obtained from Hot Water Degumming Process, J. Food Process Eng. (2015) n/a-n/a. doi:10.1111/jfpe.12267.

[48] J. Wu, Y. Zhou, S. Wang, Z. Wang, Y. Wu, X. Guo, Laboratory-scale extraction and characterization of ice-binding sericin peptides, Eur. Food Res. Technol. 236 (2013) 637–646. doi:10.1007/s00217-013-1919-8.

[49] K. Mase, T. Iizuka, E. Okada, K. Nakajima, Y. Tamura, T. Miyazima, T. Yamamoto, Breeding of the Silkworm Race "Sericin Flavo" for Production of Sericin Cocoons Containing Flavonol, J Insect Biotechnol Sericol. 77 (2008) 171–174. doi:10.11416/jibs.77.3_171.

[50] K. Mase, E. Okada, T. Uzuka, T. Yamamoto, SERICINA: DAL BACO DA SETA AI COSMETICI, Statew. Agric. L. Use Baseline 2015. 1 (2015) 2010. doi:10.1017/CBO9781107415324.004.

[51] M.N. Padamwar, A.P. Pawar, A. V Daithankar, K.R. Mahadik, Silk sericin as a moisturizer: an in vivo study., J. Cosmet. Dermatol. 4 (2005) 250–257. doi:10.1111/j.1473-2165.2005.00200.x.

[52] N. Kato, S. Sato, A. Yamanaka, H. Yamada, N. Fuwa, M. Nomura, Silk protein, sericin, inhibits lipid peroxidation and tyrosinase activity., Biosci. Biotechnol. Biochem. 62 (1998) 145–7. doi:10.1271/bbb.62.145.

[53] D.M. Nair, Biodegradable Hydrogels From Silk Sericin & Gelatin : Development and Characterization for Medical Applications, (2015).

[54] S. Nayak, T. Dey, D. Naskar, S.C. Kundu, The promotion of osseointegration of titanium surfaces by coating with silk protein sericin, Biomaterials. 34 (2013) 2855–2864. doi:10.1016/j.biomaterials.2013.01.019.

[55] S. Nayak, S. Dey, S.C. Kundu, Skin Equivalent Tissue-Engineered Construct: Co-Cultured Fibroblasts/ Keratinocytes on 3D Matrices of Sericin Hope Cocoons, PLoS One. 8 (2013) 1–17. doi:10.1371/journal.pone.0074779.

[56] L. Lamboni, M. Gauthier, G. Yang, Q. Wang, Silk sericin: A versatile material for tissue engineering and drug delivery, Biotechnol. Adv. (2015). doi:10.1016/j.biotechadv.2015.10.014.

[57] B.J. Allardyce, R. Rajkhowa, R.J. Dilley, M.D. Atlas, J. Kaur, X. Wang, The impact of degumming conditions on the properties of silk films for biomedical applications, Text. Res. J. (2015). doi:10.1177/0040517515586166.

[58] Y. Okazaki, H. Tomotake, K. Tsujimoto, M. Sasaki, N. Kato, Consumption of a Resistant Protein, Sericin, Elevates Fecal Immunoglobulin A, Mucins, and Cecal Organic Acids in Rats Fed a High-Fat Diet, J Nutr. 141 (2011) 1975–1981. doi:10.3945/jn.111.144246.1975.

[59] D. Gupta, A. Agrawal, A. Rangi, Extraction and characterization of silk sericin, Indian J. Fibre Text. Res. 39 (2014) 364–372.

[60] R. Rajendran, C. Balakumar, R. Sivakumar, T. Amruta, N. Devaki, Extraction and application of natural silk protein sericin from Bombyx mori as antimicrobial finish for cotton fabrics, J. Text. Inst. 103 (2012) 458–462. doi:10.1080/00405000.2011.586151.

[61] D. Gupta, A. Agrawal, H. Chaudhary, M. Gulrajani, C. Gupta, Cleaner process for extraction of sericin using infrared, J. Clean. Prod. 52 (2013) 488–494. doi:10.1016/j.jclepro.2013.03.016.

[62] M.L. Gimenes, V.R. Silva, M.G. a. Vieira, M.G.C. Silva, A.P. Scheer, High Molecular Sericin from Bombyx mori Cocoons: Extraction and Recovering by Ultrafiltration, Int. J. Chem. Eng. Appl. 5 (2014) 266–271. doi:10.7763/IJCEA.2014.V5.391.

[63] J. Wu, Z. Wang, S.Y. Xu, Preparation and characterization of sericin powder

extracted from silk industry wastewater, Food Chem. 103 (2007) 1255–1262. doi:10.1016/j.foodchem.2006.10.042.
[64] R. Dash, S. Mukherjee, S.C. Kundu, Isolation, purification and characterization of silk protein sericin from cocoon peduncles of tropical tasar silkworm, Antheraea mylitta, Int. J. Biol. Macromol. 38 (2006) 255–258. doi:10.1016/j.ijbiomac.2006.03.001.
[65] R. Chollakup, W. Smitthipong, K. Mougin, M. Nardin, Characterization of Sericin Biomaterial from Silk Cocoon Waste, Mater. Sci. Appl. 1 (2015) 45–50.
[66] C. Álvarez, C. Arredondo, A.E. Casas, M.M. Cardona, G.A. Hincapié, A. Restrepo-osorio, Caracterización de sericina obtenida a partir de aguas de desengomado de seda natural Characterization of sericin obtained from water degumming natural silk, Prospectiva. 11 (2013) 7–12.
[67] T.-T. Cao, Y.-Q. Zhang, Processing and characterization of silk sericin from Bombyx mori and its application in biomaterials and biomedicines, Mater. Sci. Eng. C. 61 (2015) 940–952. doi:10.1016/j.msec.2015.12.082.
[68] H. Teramoto, T. Kameda, Y. Tamada, Preparation of gel film from Bombyx mori silk sericin and its characterization as a wound dressing., Biosci. Biotechnol. Biochem. 72 (2008) 3189–3196. doi:10.1271/bbb.80375.
[69] Y.-Q. Zhang, Applications of natural silk protein sericin in biomaterials, Biotechnol. Adv. 20 (2002) 91–100. doi:10.1016/S0734-9750(02)00003-4.
[70] R. Konwarh, P. Gupta, B.B. Mandal, Silk-microfluidics for advanced biotechnological applications: A progressive review, Biotechnol. Adv. (2016) 1–14. doi:10.1016/j.biotechadv.2016.05.001.
[71] M.N. Padamwar, a. P. Pawar, Silk sericin and its applications: A review, J. Sci. Ind. Res. (India). 63 (2004) 323–329.
[72] X. Zhang, M.M.R. Khan, T. Yamamoto, M. Tsukada, H. Morikawa, Fabrication of silk sericin nanofibers from a silk sericin-hope cocoon with electrospinning method, Int. J. Biol. Macromol. 50 (2012) 337–347. doi:10.1016/j.ijbiomac.2011.12.006.
[73] Z. Wang, Y. Zhang, J. Zhang, L. Huang, J. Liu, Y. Li, G. Zhang, S.C. Kundu, L. Wang, Exploring natural silk protein sericin for regenerative medicine: an injectable, photoluminescent, cell-adhesive 3D hydrogel, Sci. Rep. 4 (2014) 7064. doi:10.1038/srep07064.
[74] M.L. Gimenes, L. Liu, X. Feng, Sericin/poly(vinyl alcohol) blend membranes for pervaporation separation of ethanol/water mixtures, J. Memb. Sci. 295 (2007) 71–79. doi:10.1016/j.memsci.2007.02.036.
[75] L.J. ZHU, M. Arai, K. Hirabayashi, Comparison of sericin characteristics between silk glands and cocoon filaments., J. Sericultural Sci. Japan. 64 (1995) 209–213.
[76] J. Passent, The molecular weight of sericin, Biochim. Biophys. Acta - Protein Struct. 147 (1967) 595–597. doi:http://dx.doi.org/10.1016/0005-2795(67)90021-9.
[77] F.R.B. Turbiani, J. Tomadon, F.L. Seixas, M.L. Gimenes, Properties and structure of sericin films: Effect of the crosslinking degree, Chem. Eng. Trans. 24 (2011) 1489–1494. doi:10.3303/CET1124249.
[78] Y.N. Jo, I.C. Um, Effects of solvent on the solution properties, structural characteristics and properties of silk sericin, Int. J. Biol. Macromol. 78 (2015) 287–295. doi:10.1016/j.ijbiomac.2015.04.004.
[79] D.E. Chung, J.H. Lee, H. Kweon, K.-G. Lee, I.C. Um, Structure and properties of silk sericin obtained from different silkworm varieties, Int. J. Ind. Entomol. 30 (2015) 81–85. doi:10.7852/ijie.2015.30.2.81.
[80] D.E. Chung, H.H. Kim, M.K. Kim, K.H. Lee, Y.H. Park, I.C. Um, Effects of different Bombyx mori silkworm varieties on the structural characteristics and properties of silk, Int. J. Biol. Macromol. 79 (2015) 943–951. doi:10.1016/j.ijbiomac.2015.06.012.
[81] H. Oh, J.Y. Lee, K.H. Lee, Effect of Salts on Gelation Time of Silk Sericin Solution, Int. J. Ind. Entomol. 27 (2013) 326–328. doi:10.7852/ijie.2013.27.2.326.
[82] H. Oh, J.Y. Lee, M.K. Kim, I.C. Um, K.H. Lee, Refining hot-water extracted silk sericin by ethanol-induced precipitation, Int. J. Biol. Macromol. 48 (2011) 32–37. doi:10.1016/j.ijbiomac.2010.09.008.
[83] Y.J. Yoo, I.C. Um, Effect of Extraction Time on the Rheological Properties of Sericin Solutions and Gels, Int J Indust Entomol. 27 (2013) 180–184.
[84] H. Kaneko, The colloidal behaviour of sericin. I, Bull. Chem. Soc. Jpn. 9 (1934) 207–221. doi:10.1246/bcsj.9.207.
[85] E. Iizuka, Conformation of silk sericine in solution, Bombyx mori L., Biochim. Biophys. Acta - Protein Struct. 181 (1969) 477–479. doi:10.1016/0005-2795(69)90284-0.
[86] H. Ishikawa, K. Hirabayashi, T. Muramatsu, The conformation of silk sericin, Sen'i Gakkaishi. 28 (1972) 167–169. doi:10.2115/fiber.28.4-5_167.
[87] D.N. Rockwood, R.C. Preda, T. Yücel, X. Wang, M.L. Lovett, D.L. Kaplan, Materials fabrication from Bombyx mori silk fibroin, Nat. Protoc. 6 (2011) 1612–1631. doi:10.1038/nprot.2011.379.
[88] Y. Song, C. Zhang, J. Zhang, N. Sun, K. Huang, H. Li, Z. Wang, K. Huang, L. Wang, An injectable silk sericin hydrogel promotes cardiac functional recovery after ischemic myocardial infarction, Acta Biomater. (2016). doi:10.1016/j.actbio.2016.05.039.
[89] C. Holland, A.E. Terry, D. Porter, F. Vollrath, Comparing the rheology of native spider and silkworm spinning dope., Nat. Mater. 5 (2006) 870–874. doi:10.1038/nmat1762.
[90] K. Kataoka, I. Uematsu, Studies on liquid silk VI - on the viscosity of liquid silk in the silkgland, Kobunshi Ronbunshu. 34 (1977) 7–13. doi:10.1295/koron.34.7.
[91] J. Sparkes, C. Holland, Analysis of the pressure requirements for silk spinning reveals a pultrusion dominated process, Nat. Commun. 8 (2017) 594. doi:10.1038/s41467-017-00409-7.
[92] N. Kojic, J. Bico, C. Clasen, G. McKinley, Ex vivo rheology of spider silk., J. Exp. Biol. 209 (2006) 4355–4362.
[93] P.R. Laity, C. Holland, Native Silk Feedstock as a Model Biopolymer: A Rheological Perspective, Biomacromolecules. 17 (2016) 2662–2671. doi:10.1021/acs.biomac.6b00709.
[94] P.R. Laity, C. Holland, Thermo-rheological behaviour of native silk feedstocks, Eur. Polym. J. (2016). doi:10.1016/j.eurpolymj.2016.10.054.
[95] P.R. Laity, C. Holland, The Rheology behind Stress-Induced Solidification in Native Silk Feedstocks, Int. J. Mol. Sci. 17 (2016) 1812. doi:10.3390/ijms17111812.
[96] J. Sparkes, C. Holland, Sericin characterisation paper data, (2017). doi:10.15131/shef.data.5198074.
[97] M.P. Escudier, I.W. Gouldson, A.S. Pereira, F.T. Pinho, R.J. Poole, On the reproducibility of the rheology of shear-thinning liquids, J. Nonnewton. Fluid Mech. 97 (2001) 99–124. doi:10.1016/S0377-0257(00)00178-6.
[98] C. Holland, D. Porter, F. Vollrath, Comparing the rheology of mulberry and "wild" silkworm spinning dopes, Biopolymers. 97 (2012) 362–367. doi:10.1002/bip.22011.
[99] Y. Takasu, H. Yamada, K. Tsubouchi, Isolation of three main sericin components from the cocoon of the silkworm, Bombyx mori., Biosci. Biotechnol. Biochem. 66 (2002) 2715–2718. doi:10.1271/bbb.66.2715.
[100] Y. Takasu, H. Yuamada, K. Tsubouchi, The silk sericin component with low crystallinity, Sanshi-Konchu Biotech. 75 (2006) 133–139.
[101] J. Michaille, P. Couble, J. Prudhomme, A. Garel, A single gene produces multiple sericin messenger-rnas in the silk gland of bombyx-mori, Biochimie. 68 (1986) 1165–1173.
[102] K. Mase, T. Iizuka, E. Okada, T. Miyajima, T. Yamamoto, A New Silkworm Race for Sericin Production,"SERICIN HOPE" and its Product,"VIRGIN SERICIN," J Insect Biotechnol Sericol. 75 (2006) 85–88.
[103] Y. Hou, Q. Xia, P. Zhao, Y. Zou, H. Liu, J. Guan, J. Gong, Z. Xiang, Studies on middle and posterior silk glands of silkworm (Bombyx mori) using two-dimensional electrophoresis and mass spectrometry, Insect Biochem. Mol. Biol. 37 (2007) 486–496. doi:10.1016/j.ibmb.2007.02.011.
[104] P. Zhang, Y. Aso, K. Yamamoto, Y. Banno, Y. Wang, K. Tsuchida, Y. Kawaguchi, H. Fujii, Proteome analysis of silk gland proteins from the silkworm, Bombyx mori, Proteomics. 6 (2006) 2586–2599. doi:10.1002/pmic.200500348.
[105] H. Teramoto, A. Kakazu, T. Asakura, Native structure and degradation pattern of silk sericin studied by 13C NMR spectroscopy, Macromolecules. 39 (2006) 6–8. doi:10.1021/ma0521147.
[106] A. Matsumoto, J. Chen, A.L. Collette, U. Kim, G.H. Altman, P. Cebe, D.L. Kaplan, Mechanisms of Silk Fibroin Sol−Gel Transitions, J. Phys. Chem. B. 110 (2006) 21630–21638. doi:10.1021/jp056350v.
[107] G. Li, P. Zhou, Z. Shao, X. Xie, X. Chen, H. Wang, L. Chunyu, T. Yu, The natural silk spinning process, Eur. J. Biochem. 268 (2001) 6600–6606. doi:10.1046/j.0014-2956.2001.02614.x.
[108] E. Iizuka, J.T. Yang, The disordered and β-conformations of silk fibroin in solution, Biochemistry. 7 (1968) 2218–2228. doi:10.1021/bi00846a026.
[109] T. Asakura, K. Okushita, M.P. Williamson, Analysis of the structure of Bombyx mori silk fibroin by NMR, Macromolecules. 48 (2015) 2345–2357. doi:10.1021/acs.macromol.5b00160.
[110] T. Asakura, Y. Watanabe, A. Uchida, H. Minagawa, NMR of Silk Fbroin.2.13C NMR Study of the Chain Dynamics and Solution Structure of Bombyx mori Silk Fibroin, Macromolecules. 17 (1984) 1075–1081.
[111] K.S. Hossain, N. Norio, J. Magoshi, Rapid Communication Rheological Study on Aqueous Solutions of Silk Fibroin Extracted from the Middle Division of Bombyx Mori Silkworm, Rapid Commun. 27 (1999) 129–130.
[112] T. Asakura, K. Umemura, Y. Nakazawa, H. Hirose, J. Higham, D.P. Knight, Some observations on the structure and function of the spinning apparatus in the silkworm Bombyx mori, Biomacromolecules. 8 (2007) 175–181. doi:10.1021/bm060874z.
[113] D.R. Picout, S.B. Ross-Murphy, Rheology of Biopolymer Solutions and Gels, Sci. World J. 3 (2003) 105–121. doi:10.1100/tsw.2003.15.
[114] S.B. Ross-Murphy, K.P. Shatwell, Polysaccharide strong and weak gels, Biorheology. 30 (1993) 217–227.
[115] C. Holland, D. Porter, F. Vollrath, Comparing the rheology of mulberry and "wild" silkworm spinning dopes, Biopolymers. 97 (2012) 362–367. doi:10.1002/bip.22011.
[116] M. Boulet-Audet, A.E. Terry, F. Vollrath, C. Holland, Silk protein aggregation kinetics revealed by Rheo-IR, Acta Biomater. 10 (2014) 776–784. doi:10.1016/j.actbio.2013.10.032.
[117] Y. Jin, Y. Hang, J. Luo, Y. Zhang, H. Shao, X. Hu, In vitro studies on the structure and properties of silk fibroin aqueous solutions in silkworm, Int. J. Biol. Macromol. 62 (2013) 162–166. doi:10.1016/j.ijbiomac.2013.08.027.
[118] T. Gamo, Genetically different components of fibroin and sericin in the mutants, Nd and Nd-s, of the silkworm Bombyx mori, Japanese J. Genet. 48 (1973) 99–104. doi:10.1266/jjg.48.99.
[119] T. Gamo, T. Inokuchi, H. Laufer, Polypeptides of fibroin and sericin secreted from the different sections of the silk gland in Bombyx mori, Insect Biochem. 7 (1977) 285–295. doi:10.1016/0020-1790(77)90026-9.
[120] T. Gamo, Genetic variants of the Bombyx mori silkworm encoding sericin proteins of different lengths, Biochem. Genet. 20 (1982) 165–177. doi:10.1007/BF00484944.
[121] V.K. Rahmathulla, Management of climatic factors for successful silkworm (Bombyx mori L.) crop and higher silk production: A review, Psyche A J. Entomol. 2012 (2012) 1–12. doi:10.1155/2012/121234.
[122] K. Kataoka, I. Uematsu, Studies on Liquid Silk VII - On the fibre formation of silk fibroin by silkworm, Kobunshi Ronbunshu. 34 (1977) 37–41. doi:10.1295/koron.34.37.
[123] C. Holland, J.S. Urbach, D.L. Blair, Direct visualization of shear dependent silk fibrillogenesis, Soft Matter. 8 (2012) 2590–2594. doi:10.1039/C2SM06886A.
[124] K. Yasuda, R.C. Armstrong, R.E. Cohen, Shear flow properties of concentrated solutions of linear and star branched polystyrenes, Rheol. Acta. 20 (1981) 163–178. doi:10.1007/BF01513059.

[125] A.E. Terry, D.P. Knight, D. Porter, F. Vollrath, pH induced changes in the rheology of silk fibroin solution from the middle division of Bombyx mori silkworm, Biomacromolecules. 5 (2004) 768–772. doi:10.1021/bm034381v.
[126] H.W. Kwak, J.E. Ju, M. Shin, C. Holland, K.H. Lee, Sericin Promotes Fibroin Silk I Stabilization Across a Phase-Separation, Biomacromolecules. (2017) acs.biomac.7b00549. doi:10.1021/acs.biomac.7b00549.
[127] Y.H. Wen, H.C. Lin, C.H. Li, C.C. Hua, An experimental appraisal of the Cox-Merz rule and Laun's rule based on bidisperse entangled polystyrene solutions, Polymer (Guildf). 45 (2004) 8551–8559. doi:10.1016/j.polymer.2004.10.012.

The rheological properties of native sericin

Supplementary information

James Sparkes[a] and Chris Holland[a,*]

b) Department of Materials Science and Engineering, The University of Sheffield, Sir Robert Hadfield Building, Mappin Street, Sheffield, S. Yorks, S1 3JD, UK

6.1. Worm raising

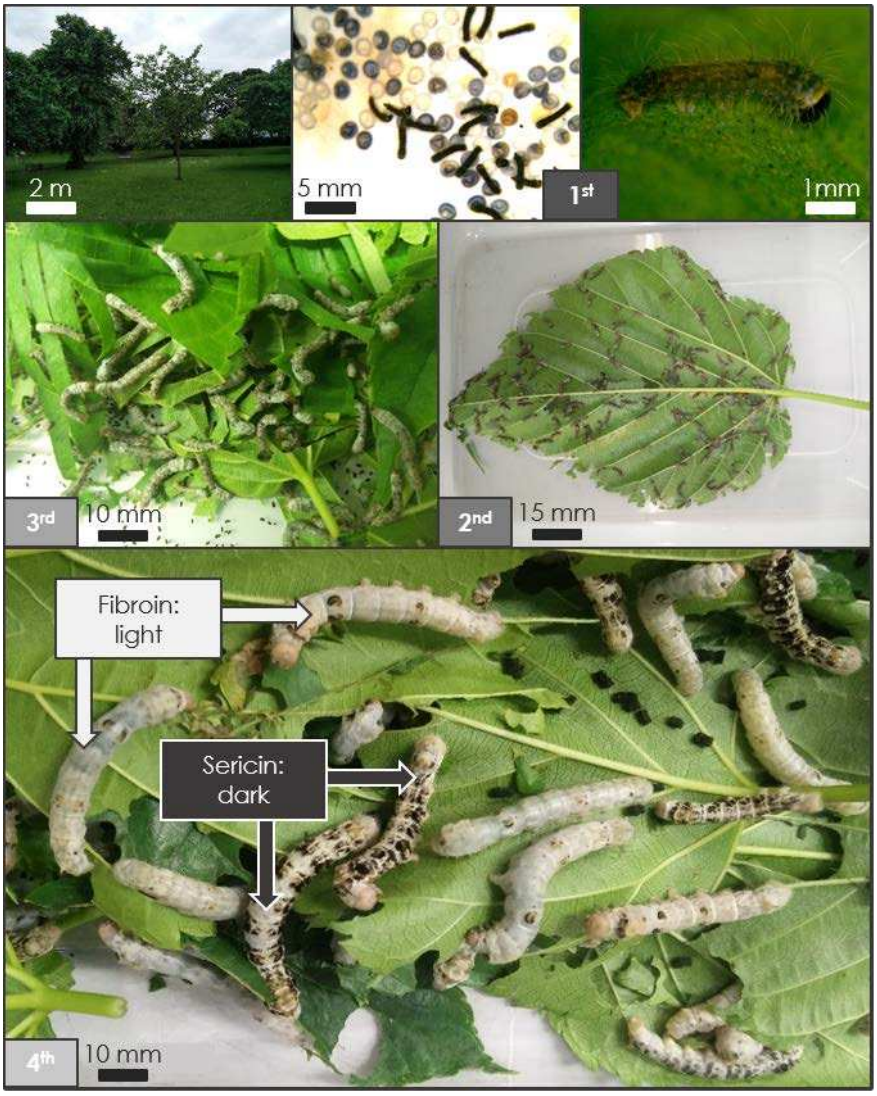

Supplementary Figure 8 – Full version of manuscript figure 1, detailing the progression from egg to 4th instar, whereupon the bimodality in the phenotype is readily observed.

6.2. Gel electrophoresis

Feedstock extracted from the silk glands of both varieties were dissolved by gently agitating in type I water over a period of several hours. Solution were diluted to 0.1 and 0.05% (mg/mg) before reduction using an equal volume of 4% (mg/mg) SDS in 4 mM 2-mercaptoethanol.

Gel electrophoresis was used to determine the molecular weights (MW) of the proteins within each sample. An SDS-PAGE system comprising a 4-20% poly-acrylamide gel was run in ambient conditions at 160V, 100mA, using an Amersham ECL Gel kit (GE Healthcare, Chicago, USA). A high molecular weight ladder ranging 30- 460kDa (HiMark, ThermoFisher Scientific, Waltham, USA) was used as the protein standard. Gels were fixed and scanned at high resolution (1200 dpi) using a photo scanner (HP Scanjet G2710). Pixel intensity was measured as a function of distance along each lane using ImageJ[1], and normalised against full lane length to allow comparison across lanes and determination of MWs.

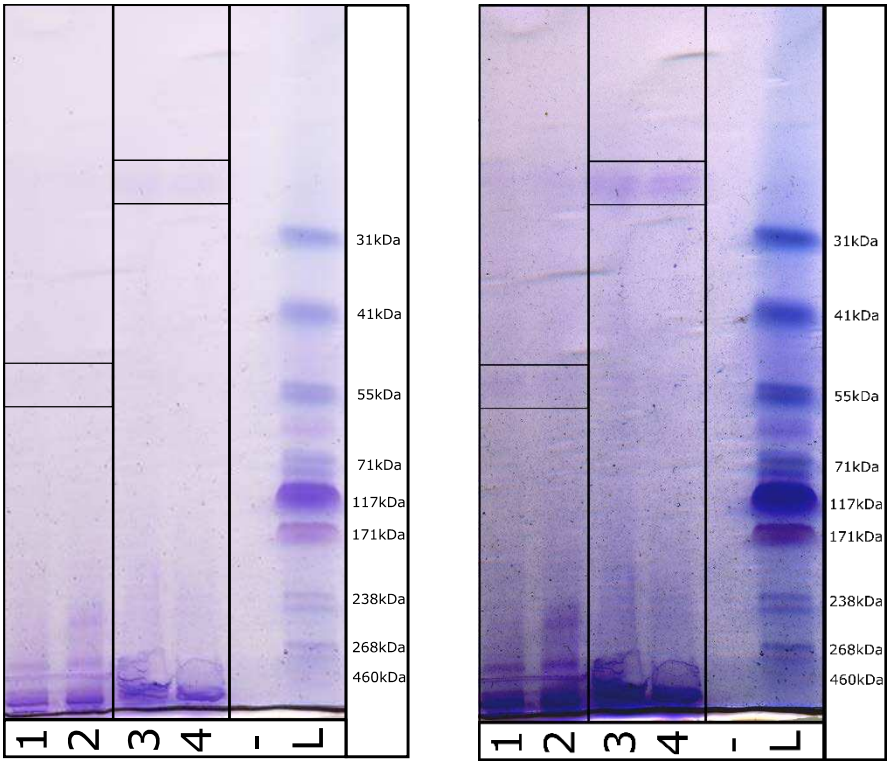

Supplementary Figure 9 – SDS-PAGE scan showing the differences in molecular weight and composition in sericin (Lanes 1 and 2) and fibroin (Lanes 3 and 4) against a ladder of known constitution (L). Fibroin shows the expected split between heavy chain at ~420kDa, and light chain at ~25kDa, whereas sericin shows several discrete regions (~400, 360, 250, 58 kDa) representing the multitude of sericin proteins present in B. mori silk glands. The left figure has been straightened, cropped and lightened, whereas the right figure has had further colour editing to the image as a whole in order to increase the contrast and better highlight the regions of interest.

6.3. Amino acid analysis

Amino acid analysis was conducted to confirm that the mutant strain was producing a feedstock consisting primarily of sericin. As can be seen in Supplementary Figure 3**Error! Reference source not found.**, the composition of the feedstock extracted from Dark specimens is remarkably similar to previously published data for sericin[2], while that produced by the Light specimens appears to be akin to fibroin of regular B. mori[2].

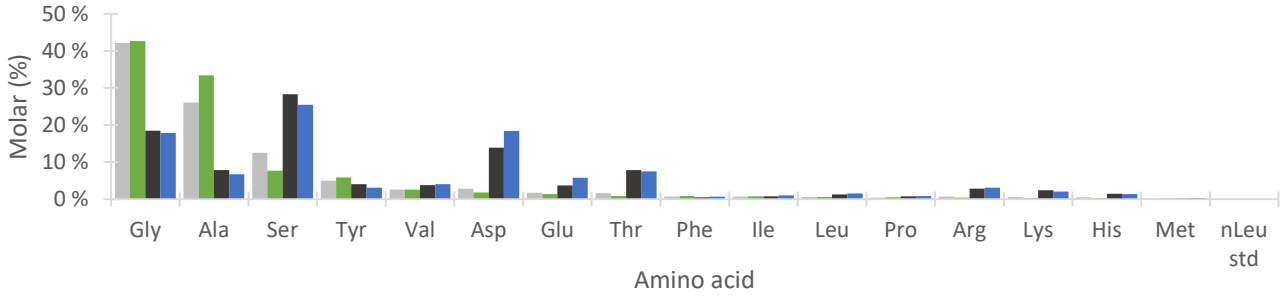

*Supplementary Figure 10 : - **Amino acid analysis** of Dark (**Black**) and Light (**grey**) silkworm feedstocks shows remarkable similarities in the composition of each when compared to previously published composition data[2] for sericin (**blue**) and fibroin (**green**) respectively. In particular, note the high proportion of serine in **Dark** specimens – the typical indicator of sericin, and the high glycine and alanine proportions typical of fibroin in **Light** specimens. Categories are ranked in order of abundance in fibroin, which highlights the distinct compositional differences between fibroin and sericin.*

Supplementary Table 2 - Summary of the Amino acid content of sericin and fibroin samples, expressed as the mean mol% from two samples. Colour scheme is reproduced from supplementary figure 2 above. Residues are ranked by order of abundance in fibroin. Dark samples are where sericin is obtained from, whereas light specimens, produce fibroin.

Mol. %	Light	Fibroin	Dark	Sericin
Gly	42.17	42.62	18.45	17.85
Ala	26.04	33.38	7.79	6.7
Ser	12.47	7.65	28.34	25.5
Tyr	5.02	5.84	4.01	3.1
Val	2.59	2.58	3.74	4.05
Asp	2.85	1.79	13.86	18.38
Glu	1.73	1.36	3.70	5.74
Thr	1.60	0.85	7.83	7.47
Phe	0.64	0.81	0.45	0.67
Ile	0.67	0.72	0.77	1.02
Leu	0.60	0.54	1.24	1.49
Pro	0.41	0.47	0.72	0.81
Arg	0.68	0.44	2.80	3.12
Lys	0.59	0.33	2.41	2.08
His	0.49	0.21	1.42	1.32
Met	0.09	0.15	0.11	0.31
sum	98.62	99.74	97.66	99.61

6.4. Spectroscopic characterisation

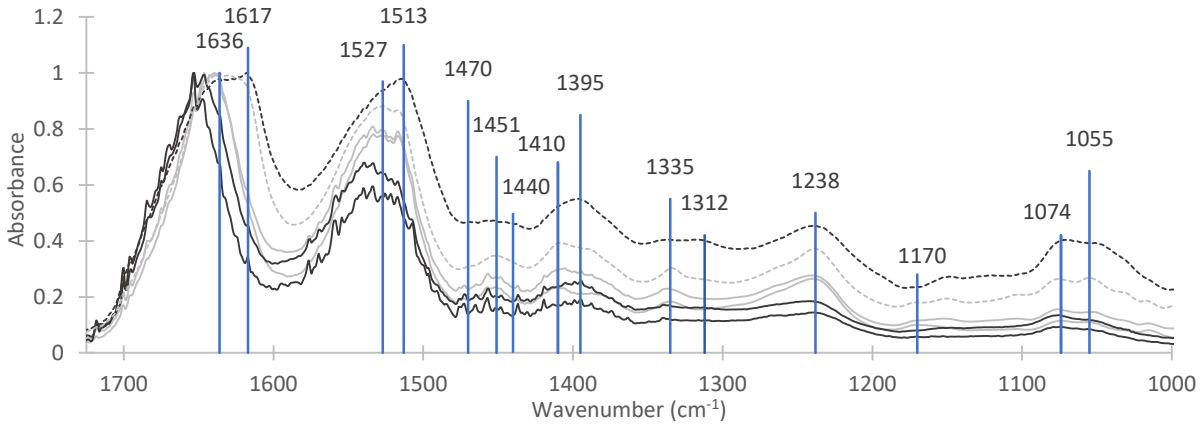

*Supplementary Figure 11- Infrared spectra of fibroin (**Dark**) and sericin (**light**) samples used for amino acid (**dashes**) and gel electrophoresis (**Solid lines**) analyses. Key peaks in the signature region are highlighted in the figure, with details and justification provided in supplementary Supplementary Table 2.*

Supplementary Table 3 - Peak assignments for sericin and fibroin, supported with justification from the literature

	wavenumber	Attributed to	Sericin supposition supported by:
Sericin peak assignment	1395	C-H bending[3]	(**1394)** Chen[4], (**1400)** Zhang's *signature sericin peak*[5], (**1384-1403)**Boulet-Audet's sericin marker band[6]
	Broad 1440-1470		Chen[4]
	1312	γ(CH2) vibrations[3]	Barth[3]
	Split **(max)** 1055/**1074**	C-C bending vibrations[3,4]	(**1041)** Barth[3], Chen[4]
	1617	Amide I	**(1637)** Chen[4] - difference due to conformational change
	1513	Amide II	**(1510)** Chen[4] - difference due to conformational change
Fibroin peak	wavenumber	Attributed to	Fibroin supposition supported By:
	1410		**(1410)** Chen[4]
	1335	CH_3 Symmetric bending	**(1334)** Chen[4]

	1451	CH_3 asymmetric bending	**(1441)** Chen[4]
	1170	N–C_α stretching[4]	Barth[3], Chen[4]
	Split **(max)** **1055**/1074	C-C bending vibrations[3,4]	(**1041)** Barth[3], Chen[4]
	1636	Amide I	**(1617)** Chen[4], **(1640-1660)** Amorphous fibroin[7–10], **(1620)** crystalline fibroin [9,11,12]
	1527	Amide II	**(1500)** Chen[4] **(1541)**Amorphous[11,12], **(1529)** crystalline[11,12]

Further confirmation of the gland contents was undertaken using FT-IR spectroscopy. Several distinct differences can be seen between the spectra. Both clearly show peaks assigned to the Amide I, II, and III bands (~1630 cm^{-1}, ~1530 cm^{-1}, and 1238 cm^{-1}) characteristic of protein structures. Comparison of *Light* and *Dark* spectra shows distinct infrared signatures, with *Light* showing many of the principal features observed in FT-IR spectra of fibroin, and *Dark* showing similarities to that of sericin. We observe substantial growth in *Dark* spectra at 1395 cm^{-1} (attributed to C-H bending[3]), which masks a peak at 1410 cm^{-1} in *Light*. This was previously assigned as Zhang's *signature sericin peak*[5], and Boulet-Audet's sericin marker band[6]. This is further validated by Chen[4], who also shows a clear peak at 1394 cm^{-1} in sericin, which appears as a lower shoulder on a peak centred at ~1410 cm^{-1} in fibroin.

Light has clear additional peak at 1335 cm^{-1}, and defined peak at 1451 cm^{-1}, both of which were observed by Chen[4] in fibroin at 1334 cm^{-1} and 1441 cm^{-1} – symmetric and asymmetric bending modes of CH_3 respectively, but not sericin. *Dark* has comparatively broad, flat peak spanning 1440-1470 cm^{-1}, again observed only in sericin and not fibroin by Chen[4]. A further peak visible at 1312 cm^{-1}in the *Dark* spectrum (also visible in Chen, unlabelled) may be assigned to γ(CH2) vibrations in sericin[3], while *Light* has an additional peak at 1170 cm^{-1}which is assigned to N–C_α stretching[4].

The split peak observed at 1055/1074 cm^{-1} is skewed toward 1074 cm^{-1} in *Dark,* and 1055 cm^{-1} in *Light,* and compares favourably with 1041 cm^{-1} peak structures observed in spectra for sericin/fibroin and assigned to C-C bending vibrations[3,4]. Chen[4] assigns further small peaks in the low wavenumber region to β-sheet formations in fibroin, which are not particularly evident in our spectra, though their samples were sheared to form films, rather than evaporated to dryness, which may account for this difference.

Amide I peak lies at 1636 cm^{-1} in the *Light* spectrum, but at 1617 cm^{-1} in the *Dark.* Amide II peak also differs from 1527 cm^{-1} in *Light* to 1513 cm^{-1} in *Dark.* This differs from previous data[4] that offered amide I peaks at 1637 cm^{-1} & 1617 cm^{-1}, and amide II at 1510 cm^{-1} & 1500 cm^{-1}, for sericin and fibroin respectively. For fibroin this discrepancy can be attributed to the film production methods, as amorphous silk fibroin is shown to have an amide I peak In the region of 1640-1660 cm^{-1} [7–10], whereas increasing the β-sheet content (through methanol treatment or similar) reduces this peak to ~1620 cm^{-1} [9,11,12]. A similar shift is observed in the Amide II band, moving from 1541 to 1529 cm^{-1} [11,12]. We suggest that the differences between sericin's[4] and *Dark's* spectra are due to conformational change arising from the difference between native and recovered sericin.

The FT-IR spectra of samples used in SDS-PAGE show the same signatures as those used in amino acid analysis, which provides a link between the three techniques. Further to this, the analysis of both glands from a single specimen allows

the variation between glands to be examined. Spectra from both glands of a single specimen proved to be remarkably similar, allowing us to choose the gland which was best preserved after dissection for use in further work.

6.4.1. Summary

In brief, we believe that we have carried out sufficiently broad material characterisation, and that the widespread agreement between amino acid analysis, FT-IR spectra, and gel electrophoresis results justifies focussing our research efforts on the further characterisation of the feedstocks found in the *Dark* variants of the *Nd-s B. mori* strain, which we firmly believe to be primarily composed of sericin.

7. Maxwell model fitting

Although a single Maxwell model was not sufficient to represent sericin's behaviour, the literature has shown that a binary model can provide a good fit for biopolymer solutions[13] and thus the elastic and viscous moduli of individual sericin samples were curve-fitted using a binary Maxwell model ($x = 2$) of the form:

$$G'(\omega) = \sum_{i=1}^{x} \left(\frac{g_i \omega^2 \tau_i^2}{1+\omega^2 \tau_i^2} \right) \qquad G''(\omega) = \sum_{i=1}^{x} \left(\frac{g_i \omega \tau_i}{1+\omega^2 \tau_i^2} \right)$$

Where g_i represents the weighted modulus contribution of each Maxwellian element, and τ_i representing the corresponding relaxation times. Comparison between shear and oscillatory measurements was undertaken to assess cross-experimental data reliability. Through further application of the Maxwell Model[13–15]l, which states that:

$$\eta_0 = \sum_{i=1}^{\infty} g_i \tau_i$$

We can estimate the mean zero shear viscosity from oscillatory data as 46.59 Pa.s, which is comparable to that predicted by the Carreau-Yasuda model (58.63 Pa.s). Linear regression of the data sets, constrained about the origin, shows strong correlation (R^2=0.9443) for the relation $y = 1.48x$, and while the coefficient is higher than the expected value (1), this strong correlation confirms the reliability and consistency of the experimental design, suggesting that the main source of variation is biological.

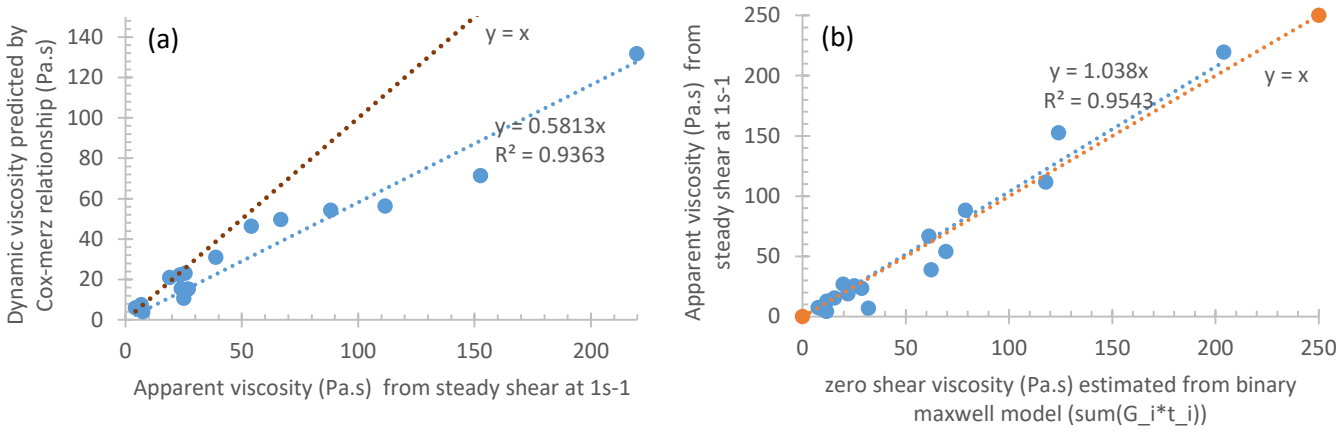

*Supplementary Figure 12 – **(a)** Comparison between zero shear viscosity estimated from the Cox-Merz relation and that measured through steady shear shows systematic underrepresentation by the predictive models. This is in stark contrast to **(b)**, which compares zero shear viscosity estimated from the binary Maxwell model to that measured through steady shear.*

7.1. Supplementary references

[1] C. a Schneider, W.S. Rasband, K.W. Eliceiri, NIH Image to ImageJ: 25 years of image analysis, Nat. Methods. 9 (2012) 671–675. doi:10.1038/nmeth.2089.

[2] T.-T. Cao, Y.-Q. Zhang, Processing and characterization of silk sericin from Bombyx mori and its application in biomaterials and biomedicines, Mater. Sci. Eng. C. 61 (2015) 940–952. doi:10.1016/j.msec.2015.12.082.

[3] A. Barth, The infrared absorption of amino acid side chains., Prog. Biophys. Mol. Biol. 74 (2000) 141–173. doi:10.1016/S0079-6107(00)00021-3.

[4] F. Chen, D. Porter, F. Vollrath, Silk cocoon (Bombyx mori): Multi-layer structure and mechanical properties, Acta Biomater. 8 (2012) 2620–2627. doi:10.1016/j.actbio.2012.03.043.

[5] X.M. Zhang, P. Wyeth, Using FTIR spectroscopy to detect sericin on historic silk, Sci. China Chem. 53 (2010) 626–631. doi:10.1007/s11426-010-0050-y.

[6] M. Boulet-Audet, F. Vollrath, C. Holland, Identification and classification of silks using infrared spectroscopy, J. Exp. Biol. 218 (2015) 3138–3149. doi:10.1242/jeb.128306.

[7] W. Surewicz, H. Mantsch, New insight into protein secondary structure from resolution-enhanced infrared spectra, Biochim. Biophys. Acta. 952 (1988) 115–130. http://cat.inist.fr/?aModele=afficheN&cpsidt=7678532.

[8] Z.H. Ayub, M. Arai, K. Hirabayashi, Quantitative structural analysis and physical properties of silk fibroin hydrogels, Polymer (Guildf). 35 (1994) 2197–2200. doi:10.1016/0032-3861(94)90250-X.

[9] X. Chen, Z. Shao, N.S. Marinkovic, L.M. Miller, P. Zhou, M.R. Chance, Conformation transition kinetics of regenerated Bombyx mori silk fibroin membrane monitored by time-resolved FTIR spectroscopy, Biophys. Chem. 89 (2001) 25–34. doi:10.1016/S0301-4622(00)00213-1.

[10] O.N. Tretinnikov, Y. Tamada, Influence of casting temperature on the near-surface structure and wettability of cast silk fibroin films, Langmuir. 17 (2001) 7406–7413. doi:10.1021/la010791y.

[11] H.-J. Jin, J. Park, R. Valluzzi, P. Cebe, D.L. Kaplan, Biomaterial films of Bombyx mori silk fibroin with poly(ethylene oxide)., Biomacromolecules. 5 (2004) 711–717. doi:10.1021/bm0343287.

[12] B.D. Lawrence, Methods to produce silk fibroin film biomaterials for applications in corneal tissue regeneration, Tufts University, 2008. doi:1450793.

[13] P.R. Laity, C. Holland, Native Silk Feedstock as a Model Biopolymer: A Rheological Perspective, Biomacromolecules. 17 (2016) 2662–2671. doi:10.1021/acs.biomac.6b00709.

[14] P.R. Laity, S.E. Gilks, C. Holland, Rheological behaviour of native silk feedstocks, Polymer (Guildf). 67 (2015) 28–39. doi:10.1016/j.polymer.2015.04.049.

[15] P.R. Laity, C. Holland, Thermo-rheological behaviour of native silk feedstocks, Eur. Polym. J. (2016). doi:10.1016/j.eurpolymj.2016.10.054.